Infrared Physics & Technology 63 (2014) 193–197

Contents lists available at ScienceDirect

Infrared Physics & Technology

journal homepage: www.elsevier.com/locate/infrared

# Effects of incident-light-intensity-dependent band gap narrowing on barrier heights of p-doped $Al_xGa_{1-x}As$/GaAs heterojunction devices

P.K.D.D.P. Pitigala, Y.F. Lao, A.G.U. Perera *

*Department of Physics and Astronomy, Georgia State University, Atlanta, GA 30303, USA*

## HIGHLIGHTS

- Light-intensity causes zero VB offsets in low-barrier IR detectors at $T > 50$ K.
- PL shows band gap increase in undoped GaAs with illumination at $T = 25$ K.
- Undoped GaAs and p-AlGaAs are reluctant to BGN caused by incident light intensity.
- Undoped GaAs/p-doped $Al_{0.01}Ga_{0.99}As$ combination suitable for FIR/THz detectors.

## ARTICLE INFO

*Article history:*
Received 3 October 2013
Available online 18 January 2014

*Keywords:*
Incident-light-intensity
FIR
THz
GaAs
AlGaAs
Band offset

## ABSTRACT

Band gaps of semiconductor materials are reduced due to band gap narrowing (BGN). Photoluminescence measurements on GaAs and AlGaAs thin films revealed a dependency of incident light intensity, and temperature in BGN in addition to the doping density. As a result, the valence band offset of p-doped GaAs/AlGaAs heterojunctions were reduced under illumination and high temperatures. We present evidence of incident-light-intensity causing barrier reduction at temperature >50 K causing zero valence band offsets in low-barrier heterostructures such as p-GaAs/$Al_{0.01}Ga_{0.99}As$, in addition to the dark-current increase by thermal excitations, causing the device failure at high temperatures.



## 1. Introduction

The motivation of this work is to understand the effects of incident photon intensity on p-doped heterojunction devices made with semiconductor materials. Carrier excitations cause changes in the occupied energy band levels in conduction or valence bands of a semiconductor material. For example, in highly n-doped semiconductors, electrons in the lower levels of the conduction band (CB) prevent carriers from further occupying those energy states; as a result, carriers have to occupy higher energy states. This phenomenon resemble an increase in the material's band gap known as the Burstein-Moss (BM) shift [1,2] when the band gap is extracted by optical methods such as absorption and photoluminescence (PL) spectra. Furthermore, band gap excitations in p-doped semiconductors cause electrons from valence band (VB) to inject on to empty states in CB. As a result, a phenomenon similar to B-M effect can be observed because the energies at the highest occupied energy level of the CB and the lowest unoccupied energy level of the VB are at further apart from where they were under dark conditions. Optoelectronic devices, based on band gap excitations or CB offset are affected by the BM effect.

Another phenomenon affecting the band offset of heterojunctions is the band gap narrowing (BGN). BGN is resulted by the ionized dopants in the doped materials, in addition to many-body interactions caused by carrier occupancy in the CB and the holes generated in the VB. Just as the occupancy of carriers in CB and VB are changing under different incident photon intensities BGN also changes based on the incident photon intensity. This implies that the occupied and unoccupied levels in CB and VB respectively will be shifted farther apart or closer to each other, depending on the magnitudes of difference between B-M and BGN under incident photon intensities. As a result, the band gap will either increase or decrease; therefore, BGN alters the response spectra of optoelectronic devices based on band gap excitations or VB offset.

Studies have revealed red shift in the response spectra due to BGN on p-doped GaAs/AlGaAs quantum well structures [3] and other types of optoelectronic devices [4]. Therefore, consideration of the BM effect and BGN effect is critical when designing detector structures for far infrared (FIR) and terahertz (THz) detection, as the detection mechanism in these devices is based on intra-band transitions of carries across small band offsets (barriers) or energy

* Corresponding author. Tel.: +1 4044136037.
*E-mail address:* uperera@gsu.edu (A.G.U. Perera).

1350-4495/$ - see front matter © 2014 Elsevier B.V. All rights reserved.
http://dx.doi.org/10.1016/j.infrared.2014.01.005

gaps. Additionally the BM and BGN effects can cause a significantly larger shift in the detectors' response range from its intended response range. In the case of large shift in a FIR/THz detector, the device may not function because the barrier becomes extremely small and the thermal excitations have increased.

In Section 2 we present the experimental methods, and in Section 3 we are presenting a comparison of band gap calculated by PL measured under different temperatures and with two different excitation light intensities for GaAs and AlGaAs films. Discussions in the next two sections are based on the BGN and BM effects observed and presented in Section 3. Section 4 provides a comparison of VB offsets, calculated for hypothetical GaAs/AlGaAs heterojunctions with different aluminum fractions, using band gaps obtained by PL for GaAs and AlGaAs thin films. This comparison of band offsets provide a good understanding of the way that the band offset of GaAs/AlGaAs heterojunctions will react to incident photon intensities. And finally, we compare our observations on band offset of low barrier devices with the reported results on a low barrier GaAs/AlGaAs heterojunction superlattice structures in literature by Matsik et.al. [5], and Rinzan et al. [6] in Section 5.

## 2. Material parameters and band gap calculation procedure

Three GaAs and two AlGaAs thin films were used in our study and were grown using molecular beam epitaxy on a semi-insulating GaAs substrate. The sample parameters are shown in Table 1. The sample GA116 is an undoped GaAs thin film, while the GA517 and GA818 are GaAs thin films, p-doped with beryllium to $5 \times 10^{17}\ cm^{-3}$ and $8 \times 10^{18}\ cm^{-3}$ respectively. The two AlGaAs thin films, labeled as AGA1 and AGA20, consist of aluminum fractions 1% and 20% respectively, and were p-doped to $3 \times 10^{18}\ cm^{-3}$ with beryllium.

The band gaps of the GaAs and AlGaAs thin film samples were calculated using PL spectra measured under different sample temperatures from 25 K to 300 K by mounting samples on the cold finger of a closed cycle refrigerator. An argon-ion laser (488 nm) was used as the excitation light source. PL were measured under two different excitation light intensities, $\sim 60\ mW\ cm^{-2}$ and $\sim 250\ mW\ cm^{-2}$, to observe the impact of incident light intensity on the materials' band gap. The laser light intensities were calibrated using a silicon photo detector. Band gap of the material is calculated by selecting 5% of the PL peak maxima as described by Ref. [7]. The low energy edge of the PL spectrum gives the lowest energy difference between occupied level in CB and highest unoccupied level in VB, while the higher energy edge gives the energy difference between the highest occupied level in CB and lowest unoccupied level in VB [7].

The theoretical band gaps of the thin film samples under different temperatures were calculated using Eq. (1) [8].

$$\overline{E}_g = E_C - E_V - E_{BGN} = E_g(0) + \frac{\alpha T^2}{(\beta + T)} - E_{BGN} \tag{1}$$

where $\overline{E}_g$ is the total energy gap and $E_C$, $E_V$, $E_{BGN}$, are the CB, VB, and band narrowing energies respectively. $E_g(0)$ is the band gap energy at 0 K in electron volts (eV) for $Al_xGa_{1-x}As$. The two coefficients, $\alpha = -5.41 \times 10^{-4}\ eV\ K^{-1}$, and $\beta = 204$ K for GaAs [9,10]. $E_g(0)$ is the direct band gap of $Al_xGa_{1-x}As$, and is calculated using Eq. (2) [9,11].

$$E_g(0) = 1.519 + 1.155x + 0.37x^2 \tag{2}$$

The temperature dependent Fermi energy level is calculated by Eq. (3) [10],

$$E_V - E_F = kT\left(\ln\left(\frac{p}{N_V}\right) + 2^{-3/2}\left(\frac{p}{N_V}\right)\right) \tag{3}$$

where $E_V$, $E_F$, $k$, $p$, and $N_V$ are the valence band energy, Fermi energy, Boltzmann constant, doping density ($cm^{-3}$) and the density of states ($cm^{-3}$) in the valence band respectively. The temperature dependency of $N_V$, for $Al_xGa_{1-x}As$ (for $x < 0.4$) was calculated by Eq. (4b) [11], by substituting, $k, \pi, m_h^*$ (density of state effective mass), and $h$ (plank constant) in Eq. (4a) [10].

$$N_V = 2\left(\frac{2\pi m_h^* kT}{h^2}\right)^{3/2} \tag{4a}$$

$$N_V = 4.82 \times 10^{15} T^{\frac{3}{2}} (0.51 + 0.25x)^{\frac{3}{2}} (cm^{-3}) \tag{4b}$$

Band gap narrowing of a material depends on four different interactions [12,13] caused by doping density of the material, (i) the exchange interactions, (ii) carrier-impurity interactions affect the majority carrier band, (iii) carrier–carrier or electron–hole interactions, and (iv) carrier impurity interaction affects in the minority carrier band. The band gap narrowing of p-doped $Al_xGa_{1-x}As$ is calculated by Eq. (5) [12,14], which gives $E_{BGN}$ of 20.7 meV for GaAs ($x = 0$) with the doping density ($p$) of $5 \times 10^{17}\ cm^{-3}$ at room temperature.

$$E_{BGN} = 9.71(1 + 0.09x)\left(\frac{p}{10^{18}}\right)^{\frac{1}{3}} + 12.19(1 + 0.42x)\left(\frac{p}{10^{18}}\right)^{\frac{1}{4}} + 3.88(1 - 0.23x)\left(\frac{p}{10^{18}}\right)^{\frac{1}{2}} \tag{5}$$

The band gaps calculated from PL measurements are compared with the band gap calculations with Eq. (1) to differentiate the changes in band gap due to incident light intensity. Additionally, PL data were also used to analyze the band offsets at GaAs/AlGaAs interfaces and band offset variations due to incident photon intensities. Even though various ratios, from 10:90 up to 50:50 can be found in literature as the VB:CB energy offset ratio in GaAs/AlGaAs heterostructures [9] we use 40:60 ratio in our calculations because the VB offset calculated by any other ratio will give a lower value for VB offset compared to the value given by a 40:60 ratio.

**Table 1**
Summary of sample parameters.

| Sample | Material | Aluminum fraction (%) | Doping density ($cm^{-3}$) |
|---|---|---|---|
| GA116 | GaAs | – | Undoped |
| GA517 | GaAs | – | $5 \times 10^{17}$ |
| GA818 | GaAs | – | $8 \times 10^{18}$ |
| AGA1 | AlGaAs | 1 | $3 \times 10^{18}$ |
| AGA20 | AlGaAs | 20 | $3 \times 10^{18}$ |

## 3. Burstein-Moss (BM) and band gap narrowing (BGN) effects on GaAs subjected to incident light intensities and temperature

Majority of GaAs/AlGaAs heterojunction optoelectronic devices has GaAs as the emitter and AlGaAs as barriers. Hence, the BM and BGN effects due to incident-light-intensity in GaAs and AlGaAs will directly affect the device response and performance. The variations in BM and BGN under different temperatures are well understood for GaAs and AlGaAs films. But, the incident-light-intensity dependence of the two effects under different temperatures, are not available in literature. Therefore, in this section, we present our observations of BM and BGN under different temperatures and with different incident-light-intensities for GaAs and AlGaAs, which should be useful in optoelectronic device designing.

### 3.1. Temperature effects on BM and BGN

Out observations of band gaps calculated for GA517 using Eq. (1) and PL under different temperatures as shown in Fig. 1. The

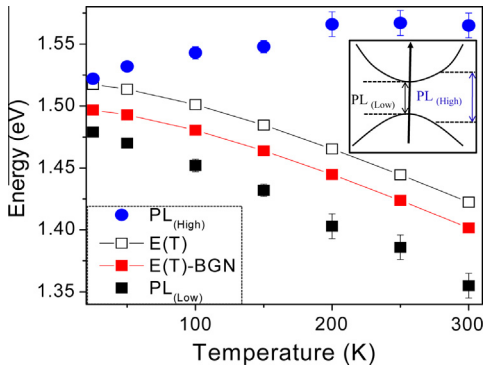


**Fig. 1.** The comparison of calculated and experimental band gaps at different temperatures from 25 K to 300 K for p-doped GaAs thin film with doping $5 \times 10^{17}$ cm$^{-3}$. E(T) is the band gap calculated without considering band gap narrowing (BGN) in Eq. (1). $PL_{(low)}$ and $PL_{(high)}$ are the band gap calculated using low and high energy slope of photoluminescence respectively E(T)-BGN is calculated band gap using Eq. (1). Inset: illustrates the calculated energies representations in a band diagram. When the sample is illuminated, carriers will be excited into the conduction band. An accumulation of charges in the CB and deprivation of carriers in VB will result in a BM shift; hence PL should have a high-energy emission. Similarly, interactions of carriers in CB and VB will result in BGN, also producing low energy photons that correspond to the lowest band gap in the material.

$PL_{(Low)}$ and $PL_{(High)}$ correspond to the band gap calculated by low and high energy slopes in PL spectra respectively. Both E(T) and E(T)-BGN are calculated using Eq. (1) by omitting and considering the BGN ($E_{BGN}$ term in Eq. (1)) respectively. As shown in the inset of Fig. 1, the low energy slope in the PL spectra corresponds to the lowest band gap. Similarly, the high energy slope defines the energy difference between the highest occupied and lowest unoccupied energy levels in the CB and VB respectively.

As expected, due to the BM effect $PL_{(High)}$ data shows higher band gap compared to the band gap calculated by Eq. (1) without considering BGN (E(T) in Fig. 1). The $PL_{(High)}$ data show increase in the band gap with increasing temperature up to ~200 K and remain constant within given error limit of ±5 eV at higher temperatures. At higher temperatures accurate determination of band gap was difficult due to low signal strength of the PL spectra; hence the error is larger compared to low temperature measurements. The deviation of $PL_{(High)}$ values from the E(T) data is a result of the BM effect.

The band gap calculated by $PL_{(Low)}$ decreases with the increasing temperature. And the increasing deviation of $PL_{(Low)}$ from E(T)-BGN with the increasing temperature implies increase in BGN with increasing temperature. Surprisingly, the band gap shown in $PL_{(Low)}$ is smaller than the value predicted by Eq. (1) (the data set E(T)-BGN in Fig. 1) with a difference ranging from ~20 meV to 40 meV as the temperature increases from 25 K to 300 K. This is due to increase in the BGN effect caused by incident-light-intensity during the PL measurement. The incident-light-intensity-dependent BGN effect is further discussed in Section 3.2. On the other hand, in Eq. (1) the temperature dependence of the BGN is not considered, this factor will also affect the difference seen between the $PL_{(low)}$ and E(T)-BGN data. In contrast, as observed by the PL data BGN will decrease at low temperatures. This should be reflected in a correction term to Eq. (1), implies the difference seen in the $PL_{(Low)}$ and E(T)-BGN is still valid.

### 3.2. Incident-light-intensity effects on BGN and MB

The variation in the band gap calculated for GA517 using low energy slope of PL spectra at 25 K, 50 K and 100 K under illumination intensities of ~60 and ~250 mW cm$^{-2}$ are shown in Table 2. A reduction in the band gap with increasing incident-light-intensity can be observed from the data in Table 2, especially at high temperature ($T$ = 100 K), which implies the temperature dependence in the BGN under illumination. At low temperatures the intensity dependence is not prominent due to carrier freezing, as the number of excitations will be inadequate. But compared to dark, illumination have carriers in the excited states resulting the difference in $PL_{(low)}$ and E(T)-BGN data as seen in Fig. 1. The BGN will be affected by an increase in the number of carries in the excited states of CB and reduction of carries in the VB due to excitations. This increase in the electron and hole density in CB and VB respectively and increase the interaction forces effecting the BGN. Additionally, the BM effect also increases with high-intensity illumination compared to low-intensity. But at higher temperatures, $T$ > 200 K, the error in band gap calculation is greater than the shift due to MB effect; therefore make it difficult to identify the intensity dependence on BM effect.

### 3.3. Effects of doping densities and material's band gap on incident-light-intensity dependent BGN

The band gaps calculated for GA818, GA116, AGA1 and AGA20 at 25 K by PL excited by 60 and 250 mW cm$^{-2}$ illuminations and calculated using Eq. (1) with and without considering BGN are presented in Table 3. Data from GA818, GA116 and GA517 were analyzed to identify the impact of doping densities on BGN under illumination intensities. Additionally, AGA1 and AGA20 were analyzed to acquire details in impact of material's band gap on BGN under illumination.

For all samples band gap calculated by $PL_{(Low)}$ are lower than the band gap calculated mathematically using Eq. (1). GA818, GA517 and GA116 show increasing band gap as the dopants density reduces. The GA818 has a lower band gap compared to the other two low doped samples, GA116 and GA517, where the difference is ~27 meV and ~25 meV at 25 K resulted by BGN due to high number of dopants in GA818. The band gap of GA818 is decreased further by ~5 meV with 250 mW cm$^{-2}$ intensity illumination. The interesting observation on the band gaps of low doped samples is that both the samples shows an increase in the band gap by ~2–3 meV when expose to 250 mW cm$^{-2}$ light intensity compared to the 60 mW cm$^{-2}$, which is different from what is observed for the high doped GaAs thin film (GA818).

Then consider the illumination-intensity effects on BGN for two AlGaAs thin films, the AGA1 with 1% aluminum fraction show a decrease in the band gap by ~4 meV with illumination-intensity of 250 mW cm$^{-2}$ compared to 60 mW cm$^{-2}$. Even though a higher band gap is expected in AGA1 compared to the GaAs samples, the band gap of AGA1 is smaller than the band gap of AG116 and AG 517 by ~11 meV and 9 meV respectively due to BGN caused by higher doping in AGA1. On contrast, the band gap of AGA20 was not changed with the incident-light intensity due to the high band gap in the AGA20.

These results show BGN variations in GaAs due to incident-light intensity are dependent on doping density. Higher doped GaAs are more susceptible to effects of incident-light-intensity on BGN. Additionally, the results of AlGaAs samples reveal the dependence of the material's band gap on BGN variations caused by incident-light intensity and can be conclude that higher band gap materials are more susceptible to BGN effect of incident-light intensity.

## 4. Effects of light Intensity on valence band offset of optoelectronic device (p-GaAs/p-AlGaAs)

The above results show that band gap alternations in materials under varying incident-light intensities are dependent on the doping density and band gap of the material. These band gap alterations under varying incident-light intensities result in band

**Table 2**
The variation in the band gap for GA517, at 25 K, 50 K and 100 K calculated by low energy slope of PL spectra under illumination intensities of ~60 and 250 mW cm$^{-2}$.

| Incident-illumination intensity (mW cm$^{-2}$) | Band gap (eV) for GA517 | | |
|---|---|---|---|
| | 25 K | 50 K | 100 K |
| 60 | 1.481 ± 0.001 | 1.472 ± 0.001 | 1.469 ± 0.002 |
| 250 | 1.483 ± 0.001 | 1.471 ± 0.001 | 1.461 ± 0.002 |

**Table 3**
The band gap calculated by PL for GA818, GA116, AGA20 and AGA1 at 25 K under the illumination of 60 and 250 mW cm$^{-2}$ and by Eq. (1) with (E(T)-BGN) and without (E(T)) bang gap narrowing effects.

| Sample | Band gap at 25 K (eV) | | | |
|---|---|---|---|---|
| | By PL | | By Eq. (1) | |
| | 60 mW cm$^{-2}$ | 250 mW cm$^{-2}$ | E(T) | E(T)-BGN |
| GA818 | 1.456 ± 0.001 | 1.451 ± 0.001 | 1.517 ± 0.0005 | 1.466 ± 0.0005 |
| GA116 | 1.483 ± 0.001 | 1.486 ± 0.001 | 1.517 ± 0.0005 | 1.496 ± 0.0005 |
| AGA20 | 1.670 ± 0.001 | 1.670 ± 0.001 | 1.763 ± 0.0005 | 1.752 ± 0.0005 |
| AGA1 | 1.472 ± 0.001 | 1.468 ± 0.001 | 1.529 ± 0.0005 | 1.492 ± 0.0005 |

offsets to be differ in heterojunction optoelectronic devices, and hence change the response spectrum of the devices. To further examine the effects, we estimated the VB offsets of two p-doped AlGaAs/GaAs heterojunctions, with (a) 20% and (b) 1% aluminum in respective barriers, using the band gaps extracted from Eq. (1) and PL spectra, for the three thin film samples GA517, AGA20 and AGA1.

For the structure with 20% aluminum barrier (i.e., assuming junction made with GA517/AGA20), the valence band offset calculated by PL is 76.4 ± 1 meV and the band offsets calculated by Eq. (1) is 91.3 meV at 25 K, rendering a difference of ~15 meV in the barrier offset estimated using PL and Eq. (1) as expected by earlier observations on BGN. This indicates that the devices will have a long wavelength threshold than what it is designed for while exposed to illumination and operating at low temperatures. In the high barrier device, the tolerance may be in an acceptable range depending on the required operational accuracy. As one aspect the long wavelength threshold can be used as an advantage in the device.

But the predicament arises in the structure with 1% aluminum in the barrier (i.e., junction made with GA517/AGA1), as can be seen in Fig. 2, the theoretical data by Eq. (1) shows a band offset of −1.8 meV (the negative barrier height indicate the higher band gap energy at the GaAs layer, caused by BGN due to higher p-doping in the AGA1 compared to GA517) and the band offset calculated by PL is −2.4 ± 1 and −2.8 ± 1 meV for the temperatures 50 K and 25 K respectively. The difference in band offset between theoretical (1.8 meV) and existing values (2.4 or 2.8 meV depending on the temperature) results in the response threshold to blue-shifted and the device not functioning in the expected wavelength spectrum. Agonizingly, at higher temperatures, the structure do not show a significant band offset (VB offset <0.5 meV). Hence the device will not have a photo response, and can only function as a resistor under bias. This result clearly indicates that devices with small band offsets are required to operate at low temperatures to maintain their barrier offset under illumination. Additionally, results conclude that not only the thermal excitation of carriers, the barrier lowering in the device too contribute to the failure in the low barrier devices, when operating at high temperatures.

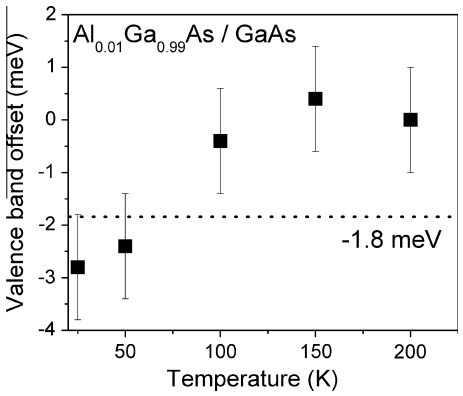


**Fig. 2.** The variation of valence band offset for p-doped AlGaAs/GaAs heterojunctions assuming 60:40 band alignment at AlGaAs:GaAs interface and band gap extracted by PL spectra with 250 mW cm$^{-2}$ incident photon intensity. The dotted line represents the band offset 1.8 meV, extracted from Eq. (1). The negative band offset indicates the GaAs layer has the higher energy.

## 5. Comparison of valence band offset on optoelectronic device with low barrier (GaAs/p-AlGaAs)

In this section we provide a comparison of the band offset calculated by PL by us in this study with a device, a terahertz (THz) detector, consists of undoped GaAs barriers and p-doped $Al_{0.01}Ga_{0.99}As$ emitters operating at 4.2 K successfully demonstrated by Matsik et al. [5]. The expected band offset obtained by response threshold for the device is 15 ± 0.1 meV as reported by Matsik et al. In this device the band off set at the GaAs/$Al_{0.01}Ga_{0.99}As$ interface is ~5.3 meV ($x * 530$ meV) and the deficit of ~9 meV is resulted by the residual doping in the GaAs barrier [5]. The band gap calculated by $PL_{(Low)}$ for p-$Al_{0.01}Ga_{0.99}As$ and undoped GaAs thin films at 25 K shown in Table 2 gives the VB band offset as ~5.8 ± 0.2 meV (PL spectra at 4.2 K is not available due to instrument limitations) closely agrees with the band offset at the interface reported by Matsik et al. The residual doping effect observed and reported by Matsik et al., can be the cause of band gap increasing observed in the PL measurement of GA116 and GA517 under increased intensity (see Table 2) presented in Section 3.3. This implies that the materials used for FIR and THz detectors should be with low doping densities. Furthermore, the data shown in Fig. 2 indicates an increase in band offset with the decreasing temperature from 50 K to 25 K. This trend can also be expected for the p-$Al_{0.01}Ga_{0.99}As$/undoped GaAs interface; hence the VB offset will be greater than 5.8 meV (at 25 K) when the temperature decreases to 4.2 K. And with the residual doping effect the actual band offset can be higher to compensate the band offset reduction caused under illumination.

Additionally, the band gap of both the undoped GaAs (GA116) and p-doped $Al_{0.01}Ga_{0.99}As$ (AGA1) shows an increase by approximately similar amount, i.e., by ~3 ± 1 meV and 4 ± 1 meV respectively under illumination of 250 mW cm$^{-2}$ compared to 60 mW cm$^{-2}$. This implies BGN under varying incident photon intensity is similar for both GA116 and AGA1, hence the barrier offsets at the undoped GaAs/p-doped $Al_{0.01}Ga_{0.99}As$ interface should not have a significant difference under varying illumination intensities. Since the effects on BGN due to carrier excitations by photon flux intensity is similar for both the materials it can be conclude

that the material combination p-$Al_{0.01}Ga_{0.99}As$ and undoped GaAs using as emitter and barrier will be more reluctant to the barrier height alternations caused by incident-light intensities at low temperatures. Therefore, a sustainable band offset can be present in the device at low temperature. And this low sensitivity to the incident photon intensity may be the cause of successful operation of the device presented by Matsik et al., in addition to the effective barrier height increase due to residual doping in GaAs barrier can be high as 13 meV, as described by Rinzan et al. [6].

## 6. Conclusions

In this study, we present effects on BGN of GaAs and AlGaAs due to carrier excitations by incident-light intensity. As a result, the band offset at the GaAs/AlGaAs interface of heterojunction structures is reduced. PL measurements were used to estimate the band gaps of GaAs and AlGaAs. Excitation light intensities of 60 and 250 mW $cm^{-2}$ are used to illustrate the alternations in BGN due to incident light intensity. Our PL spectra measured on GaAs and AlGaAs thin films revealed a dependency of incident light intensity, temperature, doping density and the material's band gap in BGN. Due to the incident-light-intensity dependence in BGN, the VB offset of p-doped GaAs/AlGaAs heterojunctions are altered when the junction is illuminated. This BGN effect has great impact on low-barrier devices with long wavelength response such as terahertz and far infrared detectors. We have presented evidence of incident-light-intensity-dependent BGN causing barrier reduction at higher temperatures ($T > 50$ K), leading low barrier structures, such as p-GaAs/$Al_{0.01}Ga_{0.99}As$, to have zero valence band offset. In addition to device failure caused by increased dark current due to thermal excitations at high temperatures, this band offset reduction too is a cause of the device failure at high temperatures. Additionally undoped GaAs has shown a band gap increase under illumination with 250 mW $cm^{-2}$ compared to 60 mW $cm^{-2}$, which makes it a superior material to use as a barrier in low barrier heterojunction devices to prevent device failure under illumination.

## Acknowledgements

This material is based upon work supported by, or in part by, the US Army Research Laboratory and the US Army Research Office under contract/Grant Number W911NF-12-2-0035. Authors also like to thank Dr. H.C. Liu, for samples. Additionally, P.K.D.D.P. Pitigala acknowledges Dr. E.S. Lopez for her critical reading of the manuscript.

## References

[1] E. Burstein, Anomalous optical absorption limit in InSb, Phys. Rev. 93 (1954) 632–633.
[2] J.A. Lahtinen, Electroreflectance study of the Burstein-Moss shift in indium phosphide, Phys. Rev. B33 (1986) 2550–2553.
[3] D.A. Kleinman, R.C. Miller, Band-gap renormalization in semiconductor quantum wells containing carriers, Phys. Rev. B 32 (1985) 2266–2272.
[4] A.C. Ferreira et al., Optical studies of acceptor centre doped GaAs/AlGaAs quantum wells, Solid–State Electron. 40 (1996) 89–92.
[5] S.G. Matsik, M.B.M. Rinzan, A.G.U. Perera, H.C. Liu, Z.R. Wasilewski, M. Buchanan, Cutoff tailorability of heterojunction terahertz detectors, Appl. Phys. Lett. 82 (2003) 139–141.
[6] M.B.M. Rinzan, A.G.U. Perera, S.G. Matsik, H.C. Liu, Z.R. Wasilewski, M. Buchanan, AlGaAs emitter/GaAs barrier terahertz detector with a 2.3 THz threshold, Appl. Phys. Lett. 86 (2005) 071112–071113.
[7] J. Wagner, Photoluminescence and excitation spectroscopy in heavily doped n- and p-type silicon, Phys. Rev. B 29 (1984) 2002–2009.
[8] M.Z.I. Gering, K.B. White, The Burstein-Moss shift for mercury cadmium telluride, J. Phys. C: Solid State Phys. 20 (1987) 1137–1145.
[9] S. Adachi, GaAs and Related Materials; Bulk Semiconducting and Superlattice Properties, World Scientific, Singapore, 1994.
[10] S.M. Sze, K.K. Ng, in: Physics of Semiconductor Devices, John Wiley & Sons, Inc., Hoboken, New Jersey, 2007, p. 19.
[11] $Al_xGa_{1-x}As$ band structure and carrier concentration, <http://www.ioffe.ru/SVA/NSM/Semicond/AlGaAs/bandstr.html> (19.09.2013).
[12] S.C. Jain, D.J. Roulston, A simple expression for band gap narrowing (BGN) in heavily doped Si, Ge, GaAs and $Ge_xSi_{1-x}$ strained layers, Solid-State Electron. 34 (1991) 453–465.
[13] G. Mahan, Energy gap in Si and Ge: impurity dependence, J. Appl. Phys. 51 (1980) 2634–2646.
[14] H.Q. Zheng, H. Wang, P.H. Zhang, Z. Zeng, K. Radahakrishnan, S.F. Yoon, G.I. Ng, Band gap narrowing effect in Be-doped $Al_xGa_{1-x}As$ studied by photoluminescence spectroscopy, Solid-State Electron. 44 (2000) 37–40.